

Supporting Information

Symmetry-Reduction Enhanced One-Dimensional Polarization-Sensitive Photodetectors for Multi-Functional Applications

*Wei Gan^{†a}, Chentao Zhang^{†a}, Guanghui Peng^a, Liqiang Xu^a, Zihao Tong^d, Zhuxin Zhang^d, Chuanqiang Wu^{*a}, Yang Zhou^{*b}, Zhen Wang^{*c}*

- a. Institute of Physical Science and Information Technology and Information Materials and Intelligent Sensing Laboratory of Anhui Province, Anhui University, Hefei 230601, China
- b. Songshan Lake Materials Laboratory, Dongguan 523808, China
- c. State Key Laboratory of Infrared Physics, Shanghai Institute of Technical Physics, Chinese Academy of Sciences, Shanghai 200083, China
- d. Stony Brook Institute at Anhui University, Anhui University, Hefei 230039, China

Keywords: one dimensional (1D) van der Waals (vdW) material, broadband photoresponse, polarization sensitivity, convolutional processing, multiplexing optical communications

*Email: wucq@ahu.edu.cn, zhouyang@sslab.org.cn, wangzhen@mail.sitp.ac.cn

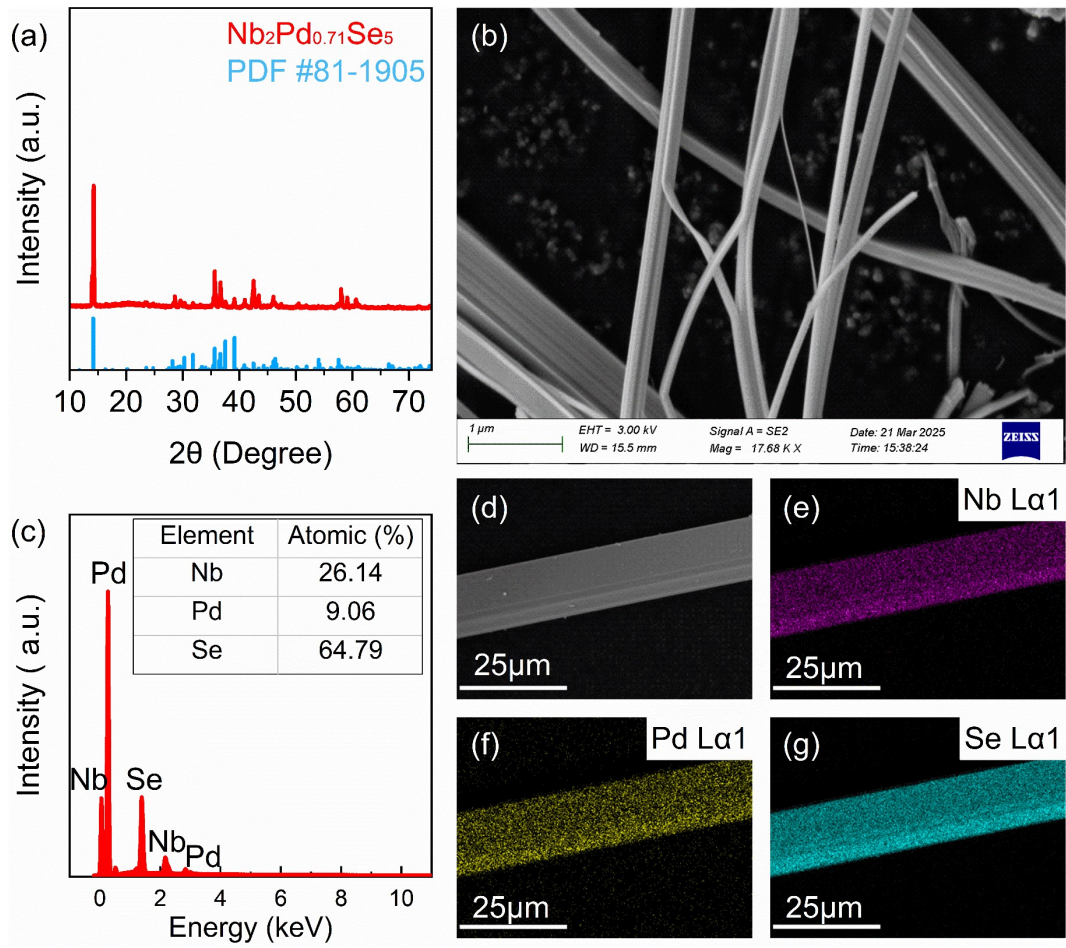


Figure S1 (a) XRD pattern of the as-synthesized $\text{Nb}_2\text{Pd}_{0.71}\text{Se}_5$ single crystal. (b) SEM of the $\text{Nb}_2\text{Pd}_{0.71}\text{Se}_5$ single crystal. (c) EDS spectrum of the $\text{Nb}_2\text{Pd}_{0.71}\text{Se}_5$ single crystal. (d) SEM image, (e) Nb element mapping, (f) Pd element mapping, and (g) Se element mapping of the $\text{Nb}_2\text{Pd}_{0.71}\text{Se}_5$ single crystal.

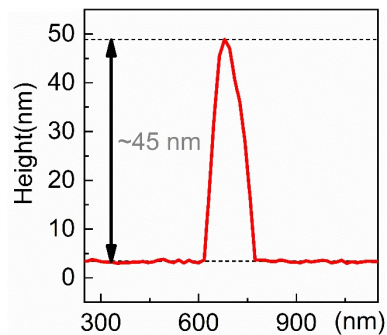


Figure S2 The atomic force microscope (AFM) height profile of the as-exfoliated $\text{Nb}_2\text{Pd}_{0.71}\text{Se}_5$, showing the diameter of $\sim 45 \text{ nm}$.

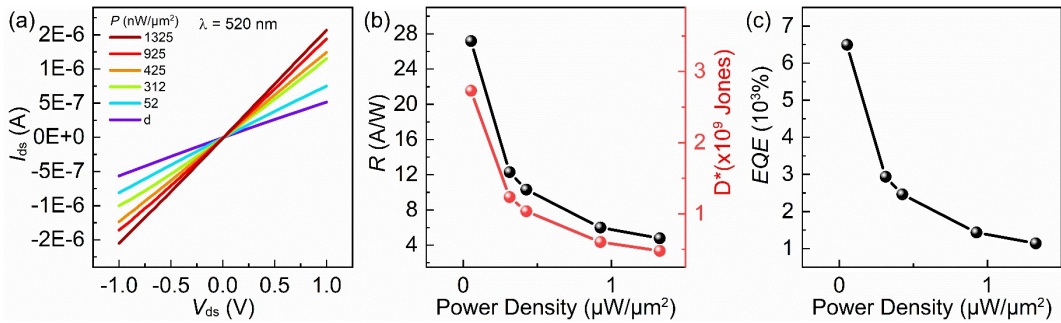


Figure S3 Photoresponse of the 1D vdW $\text{Nb}_2\text{Pd}_{0.71}\text{Se}_5$ photodetector under 520 nm laser irradiation with various power densities ranging from 52 to 1325 nW/ μm^2 and 1 V bias voltage. (a) Linear output characteristics of the device under illumination with various power densities. (b) Responsivity (R) and Specific detectivity (D^*), (c) External quantum efficiency (EQE) of the device as functions of the laser power density.

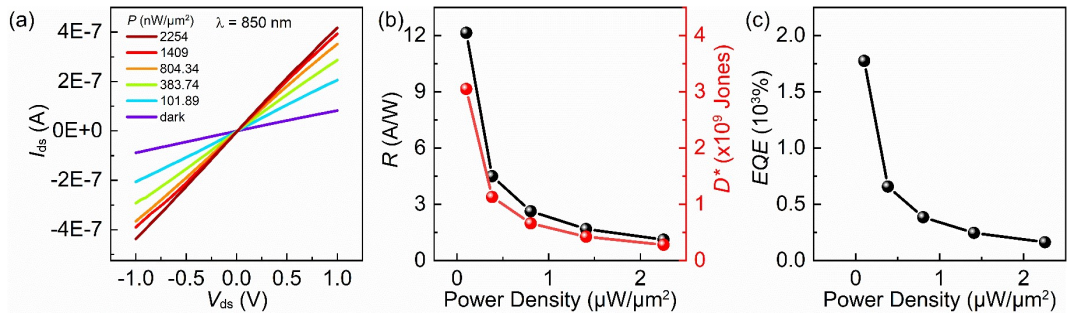


Figure S4 Photoresponse of the 1D vdW Nb₂Pd_{0.71}Se₅ photodetector under 850 nm laser irradiation with various power densities ranging from 101.89 to 2254 nW/μm² and 1 V bias voltage. (a) Linear output characteristics of the device under illumination with various power densities. (b) Responsivity (R) and Specific detectivity (D^*), (c) External quantum efficiency (EQE) of the device as functions of the laser power density.

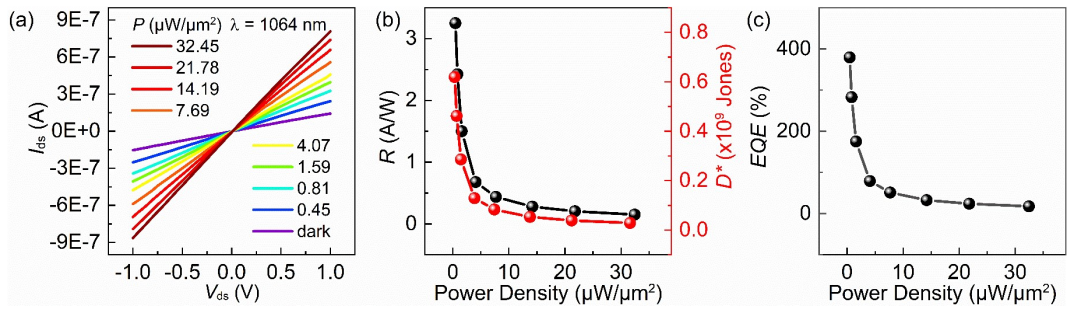


Figure S5 Photoreponse of the 1D vdW $\text{Nb}_2\text{Pd}_{0.71}\text{Se}_5$ photodetector under 1064 nm laser irradiation with various power densities ranging from 0.45 to 32.45 $\mu\text{W}/\mu\text{m}^2$ and 1 V bias voltage. (a) Linear output characteristics of the device under illumination with various power densities. (b) Responsivity (R) and Specific detectivity (D^*), (c) External quantum efficiency (EQE) of the device as functions of the laser power density.

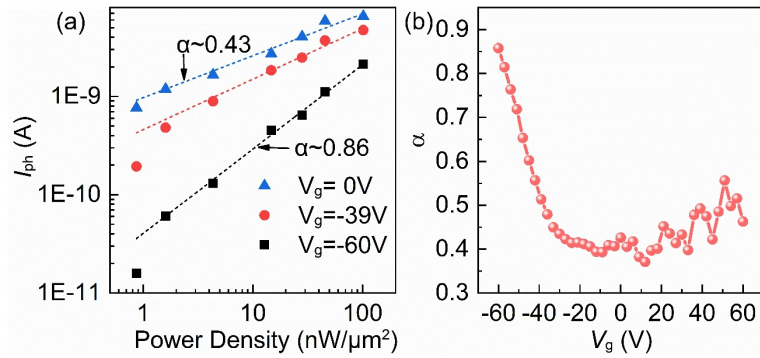


Figure S6 (a) Photocurrent as a function of power density at different gate voltages ranging from 0 V to -60 V. (b) Gate dependence of the power law coefficient (α) extracted from the fitting in (a).

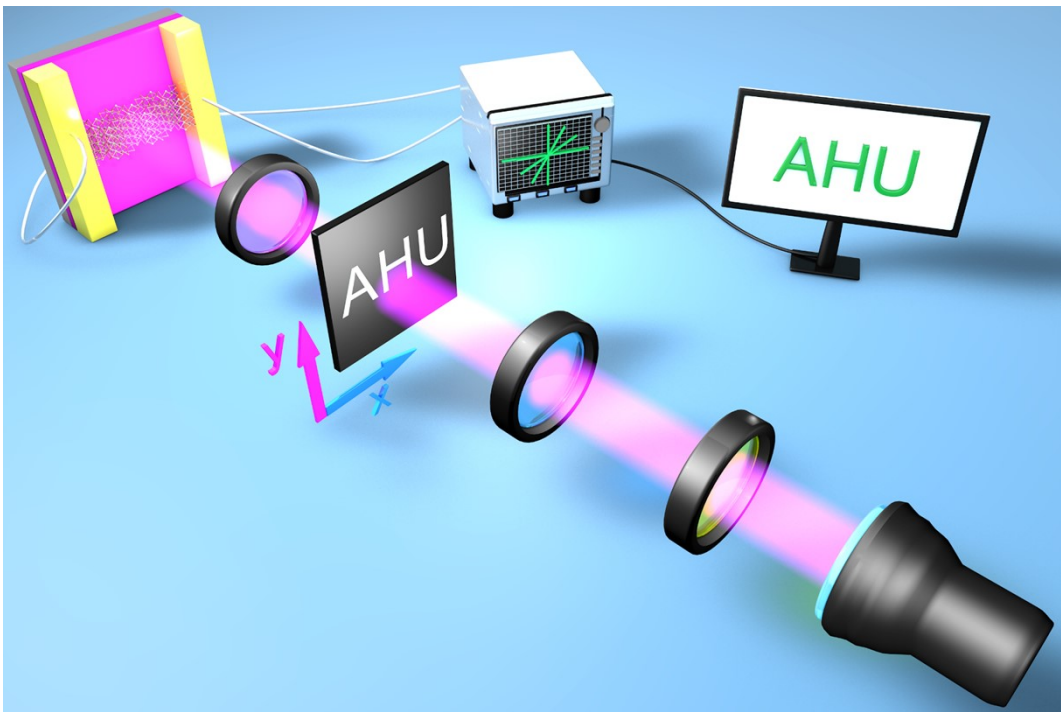


Figure S7 Experimental setup of the polarization imaging system.

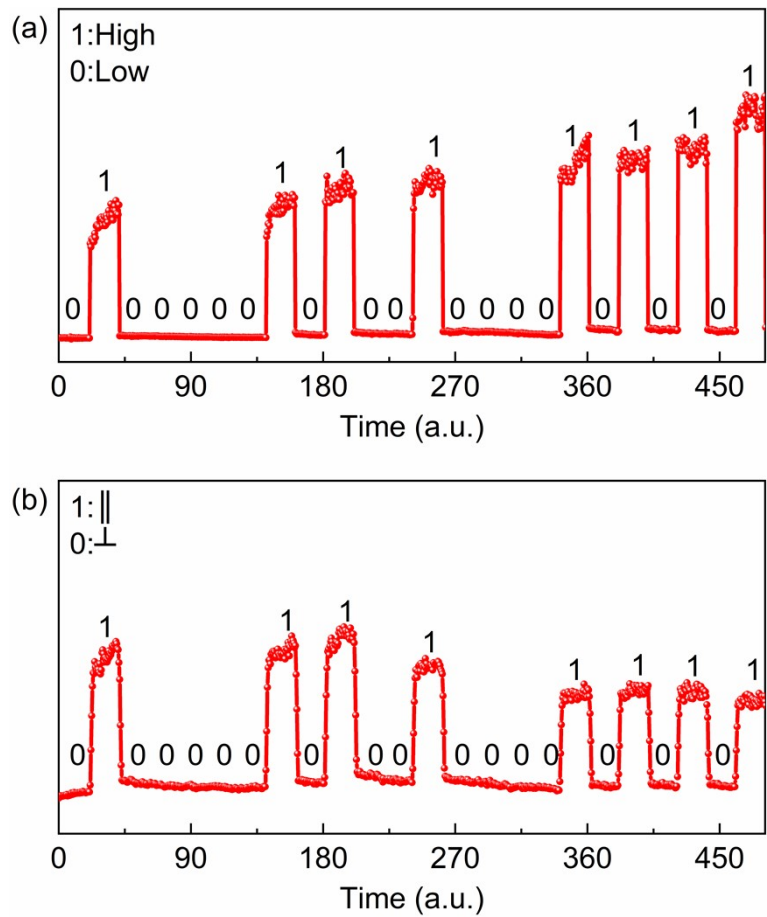


Figure S8 Information transmission of 0100000101001000 via merely (a) light intensity or (b) light polarization state, respectively. The “High” and “Low” represent the light intensity. The \leftrightarrow and \uparrow represent the parallel and perpendicular polarization states, respectively.

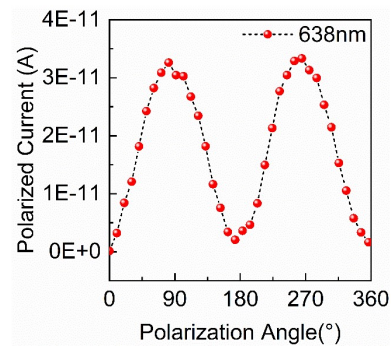


Figure S9 Polarization-sensitive photoresponse captured under 638 nm laser illumination, with the polarization angle systematically adjusted from 0° to 360°.

Table S1 Comparison of the photoresponse parameters and anisotropic ratio of $\text{Nb}_2\text{Pd}_{0.71}\text{Se}_5$ photodetector with previous reports.

Structure	R (A/W)	Rise/decay time	Anisotropy ratio	Refs
TaIrTe ₄	20 $\mu\text{A}/\text{W}$ @ 10.6 μm	τ_r : 27 μs	1.88 @ 10.6 μm	¹
Ta ₂ NiSe ₅	44 A/W @ 1064 nm	τ_r : 98 ms τ_d : 82 ms	3.24 @ 1064 nm	²
PdPS	1000 A/W @ 532 nm	τ_r : 1.4 ms τ_d : 1.2 ms	3.7 @ 808 nm	³
Sb ₂ S ₃	0.34 A/W @ 450 nm	τ_r : 470 μs τ_d : 680 μs	2.54 @ 638 nm	⁴
In ₂ SnS ₄	93.4 mA/W @ 532 nm	τ_r : 20 μs τ_d : 20 μs	1.7 @ 650 nm	⁵
Bi ₂ S ₃	673.3 A/W @ 532 nm	τ_r : 1 ms τ_d : 4.5 ms	2.4 @ 405 nm	⁶
KNb ₃ O ₈	30 A/W @ 254 nm	τ_r : 2.5 s τ_d : 1.8 s	1.62 @ 254 nm	⁷
SbBiS ₃	7.8 A/W @ 532 nm	τ_r : 10 μs τ_d : 94 μs	1.12 @ 808 nm	⁸
CrPS ₄	137 nA/W @ 405 nm	τ_r : 2 s τ_d : 2 s	1.33 @ 405 nm	⁹
GaPS ₄	4.89 A/W @ 254 nm	τ_r : 110 ms τ_d : 50 ms	1.85 @ 254 nm	¹⁰
$\text{Nb}_2\text{Pd}_{0.71}\text{Se}_5$	1590 A/W @ 638 nm	τ_r : 2.5 μs τ_d : 2.8 μs	14.4 @ 638 nm	This work

Note S1 The key parameters of photodetectors.

The photoresponse performance of the typical photodetectors are normally evaluated by responsivity (R), detectivity (D^*), and external quantum efficiency (EQE), which can be calculated through the following equations:¹¹

$$I_{\text{ph}} = I_{\text{light}} - I_{\text{dark}}$$

$$R = I_{\text{ph}}/PS$$

$$D^* = RS^{1/2}/(2eI_{\text{dark}})^{1/2}$$

$$EQE = hcR/e\lambda$$

where I_{ph} , I_{light} , P , S , e , I_{dark} , h , c , and λ represent the photocurrent, current under illumination, incident light power density, functional area, electron charge, dark current, Planck constant, light velocity, and incident light wavelength, respectively.

References

- 1 Lai, J.; Liu, Y.; Ma, J.; Zhuo, X.; Peng, Y.; Lu, W.; Liu, Z.; Chen, J.; Sun, D., *ACS Nano* 2018, **12**, 4055-4061.
- 2 Qiao, J.; Feng, F.; Wang, Z.; Shen, M.; Zhang, G.; Yuan, X.; Somekh, M. G., *ACS Appl. Mater. Interfaces* 2021, **13**, 17948-17956.
- 3 Wang, X.; Xiong, T.; Zhao, K.; Zhou, Z.; Xin, K.; Deng, H.-X.; Kang, J.; Yang, J.; Liu, Y.-Y.; Wei, Z., *Adv. Mater.* 2022, **34**, 2107206.
- 4 Zhao, K.; Yang, J.; Zhong, M.; Gao, Q.; Wang, Y.; Wang, X.; Shen, W.; Hu, C.; Wang, K.; Shen, G.; Li, M.; Wang, J.; Hu, W.; Wei, Z., *Adv. Funct. Mater.* 2021, **31**, 2006601.
- 5 Zuo, N.; Nie, A.; Hu, C.; Shen, W.; Jin, B.; Hu, X.; Liu, Z.; Zhou, X.; Zhai, T., *Small* 2021, **17**, 2008078.
- 6 Yi, H.; Ma, C.; Wang, W.; Liang, H.; Cui, R.; Cao, W.; Yang, H.; Ma, Y.; Huang, W.; Zheng, Z.; Zou, Y.; Deng, Z.; Yao, J.; Yang, G., *Mater. Horizons* 2023, **10**, 3369-3381.
- 7 Ping, Y.; Long, H.; Liu, H.; Chen, C.; Zhang, N.; Jing, H.; Lu, J.; Zhao, Y.; Yang, Z.; Li, W.; Ma, F.; Fang, X.; Wei, Z.; Xu, H., *Adv. Funct. Mater.* 2022, **32**, 2111673.
- 8 Yang, W.; Xiong, T.; Liu, Y.-Y.; Yang, J.; Xu, Q.; Wei, Z., *Small Structures* 2022, **3**, 2200061.
- 9 Zhang, H.; Li, Y.; Hu, X.; Xu, J.; Chen, L.; Li, G.; Yin, S.; Chen, J.; Tan, C.; Kan, X.; Li, L., *Appl. Phys. Lett.* 2021, **119**.
- 10 Yan, Y.; Yang, J.; Du, J.; Zhang, X.; Liu, Y.-Y.; Xia, C.; Wei, Z., *Adv. Mater.* 2021, **33**, 2008761.
- 11 Chen, J.; Zhang, Z.; Ma, Y.; Feng, J.; Xie, X.; Wang, X.; Jian, A.; Li, Y.; Li, Z.; Guo, H.; Zhu, Y.; Cui, Q.; Shi, Z.; Xu, C., *Nano Res.* 2023, **16**, 7851-7857.